Monthly Notices of the ROYAL ASTRONOMICAL SOCIETY

MNRAS **529,** 2008–2016 (2024) https://doi.org/10.1093/mnras/stae635
Advance Access publication 2024 March 1

Search and study for meteorites analogous to Didymos

G. Massa [1,2★] E. Palomba,[1] A. Longobardo,[1★] F. Dirri,[1] M. Angrisani,[1,2] C. Gisellu,[1,2] D. Polishook,[3] A. S. Rivkin[4] and C. Thomas[5]

[1]*INAF Istituto di Astrofisica e Planetologia Spaziali, via del Fosso del Cavaliere 100, I-00133 Rome, Italy*
[2]*Department of Information Engineering, Electronics and Telecommunications (DIET), University of Rome 'Sapienza', Via Eudossiana 18, I-00184 Rome, Italy*
[3]*Faculty of Physics, Weizmann Institute of Science, Rehovot 0076100, Israel*
[4]*Johns Hopkins University Applied Physics Laboratory, Laurel, MD 20734, USA*
[5]*Department of Astronomy and Planetary Science, Northern Arizona University, Flagstaff, AZ 86011, USA*

Accepted 2024 February 28. Received 2024 February 26; in original form 2024 February 6

ABSTRACT

The Hera mission will arrive at the Didymos system to study the efficiency of momentum transfer and to further investigate the binary system in great detail after the Double Asteroid Redirection Test (DART) mission impact. We took advantage of two online data bases of meteorites spectra and of recent Didymos spectra taken before and after the DART impact. We performed the first selection based on the comparison of the band centre values of the silicate absorption bands (localized at 1 and 2 μm) between Didymos and the meteorites. The second selection was made defining a four-dimensional space parameter whose dimensions were the band depth and the slope of the two bands, normalized to Didymos values. We introduced a distance measure to find the closest meteorites to Didymos in this space. Finally, we made the last selection based on other criteria, such as the presence of different spectra of the same meteorite, the presence of different spectra from different data bases, and the comparison with the literature. The result of this work is a list of six meteorites that are the most analogous to Didymos system. We also found out that Didymos is most probably mainly composed of L/LL ordinary chondrites, with a preference for the LL sub-type. From our list of meteorites, we were able to estimate the normalized abundance of olivine and pyroxene of Didymos. Finally, a match between Didymos and OC meteorites was also found in the Mid-InfraRed (MIR) range.

Key words: instrumentation: spectrographs – methods: data analysis – meteorites, meteors, meteoroids – minor planets, asteroids: individual: (65803) Didymos.

1 INTRODUCTION

The Hera mission is under development in the Space Safety Program of the European Space Agency. The mission will follow the Double Asteroid Redirection Test (DART) mission (Michel et al. 2018) and its launch is planned for October 2024. Around late December 2026, Hera will arrive near a binary system of asteroids composed of Didymos, that is the primary asteroid, and Dimorphos, i.e. Didymos' moon, in the following referred to as Didymos system. Didymos is among a potentially hazardous asteroid with a minimum orbital intersection distance of 0.04014 au (15.6 lunar distance) from the Earth (Okada et al. 2022). Hera objectives are to investigate the subsurface and interior properties of the system and to study in detail the outcome of the kinetic impactor mission DART, thus providing extremely valuable information for asteroid impact threat mitigation, mining, and science purposes (Michel et al. 2022). The scientific goals of Hera can be resumed as follows:

(i) Make the first rendezvous of a binary near-Earth asteroid;
(ii) Characterize the surface of the Didymos system;
(iii) Map the global composition of the Didymos system;
(iv) Investigate for potential fresh un-weathered material near the crater, exposed after the DART impact, to understand possible space weathering processes that occurred on the system;
(v) Characterize dust clouds around the Didymos system;
(vi) Measure the properties of an asteroid crater formed in an impact experiment at an impact speed (≈6 km s^{-1}) that is similar to inter-asteroid collisions (Michel et al. 2022);
(vii) Unveil the origin of Dimorphos as due to either a collision of the primary asteroid with another object or to a material separation from the primary asteroid due to its fast rotation (Raducan et al. 2022).

Didymos was first classified based on its visible spectra as an Xk-type asteroid (Binzel et al. 2004a, b). Then, observations in the visible and near-infrared (VIS-NIR) range showed the presence of two prominent absorption bands at 1 and 2 μm in the spectra, which led to a new classification of Didymos as an S or Sq-type asteroid (De León et al. 2006, 2010; Cheng et al. 2018).In particular, also the spectra taken across the DART impact were classified as S-type (Polishook et al. 2023), suggesting the presence of a weathered surface (DeMeo, Binzel & Lockhart 2014) and giving a hint about

★ E-mail: giuseppe.massa@inaf.it (GM); andrea.longobardo@inaf.it (AL)

Didymos system evolution (Polishook et al. 2023). Based on this, it is probably compositionally linked to the ordinary chondrite meteorites (Dunn et al. 2013). The diameter of the primary asteroid and of its moon was estimated, through radar observations and analysis of the DRACO (an imager onboard of DART) images, to be around 770 and 150 m, respectively (Naidu et al. 2020). This implies that the light reflected from the system is mainly due to Didymos and only by ∼5 per cent to Dimorphos. After the DART impact, the light reflected from the ejecta contributes by 60–70 per cent to the overall spectrum. Didymos is close to, if not beyond, the spin rate limit for loose material to remain on the surface at the equator (Cheng et al. 2018); this reinforces the hypothesis that Dimorphos is a rubble pile asteroid composed of material coming from Didymos (Pajola et al. 2022; Polishook et al. 2023). Moreover, recent spectral observation of the Didymos system, acquired right after DART impact and dominated by Dimorphos ejecta, showed it to be very similar in shape to the observation made before the impact (Polishook et al. 2023).

Fluctuations in Didymos spectral shape were seen across and before the impact, which suggest a possible heterogeneity in its surface composition (Ieva et al. 2022; De León et al. 2023; Polishook et al. 2023).

Ieva et al. (2022) took and analysed Didymos spectra between 0.34 and 0.81 μm during its 2021 apparition. The spectra were compared to the meteorites contained in RELAB (NASA Reflectance Experiment LABoratory) through a χ^2 minimization, and the ones with lower χ^2 were chosen as representative of Didymos spectral behaviour. Ieva et al. (2022) pointed out that a VIS–NIR analysis was necessary to improve the selection.

Rivkin et al. (2023) found a mismatch between the OC meteorites and Didymos in the Mid-InfraRed (MIR) spectral range. In particular, a prominent feature is found between 10 and 10.5 μm in the Didymos spectrum that was not seen in the OC spectra. In other works (Vernazza et al. 2012; Sultana et al. 2023), the mismatch was addressed to differences in porosity or/and the presence of hyperfine particles mixed with opaque material, while the feature near 10 μm was supposed to be due to an increased contribution to the Didymos spectrum from olivine (Rivkin et al. 2023).

Ordinary chondrites are widely studied meteorites and they are mainly composed of silicates (Adams 1974; Cloutis et al. 1986, 2015; Dunn et al. 2010a). The OC class of meteorites is subdivided on the basis of chemistry into three groups, the H, L, and LL chondrites, for high total iron, low total iron, and low total iron plus low metallic iron, respectively (Grady, Pratesi & Cecchi 2014). The pyroxene and olivine presence in OCs are the causes of the 1 and 2 μm absorption bands, and the study of their spectral parameters (e.g. band centre, band depth, slope) gives a suggestion about their abundance and their composition. In particular, these absorption features arise from electronic transitions in Fe^{2+} cations located in specific crystallographic sites within the minerals, and the different structures of crystallographic sites and the presence of different atoms in them modify the shape of the absorptions. Thus, the spectral features are also diagnostic for the mineral composition and structure.

In this work, the meteorites analogous to Didymos system will be searched through a comparative spectroscopic analysis of meteorites and asteroids. This result will support the calibration and data analysis of the scientific payloads described above, as well as the prediction and support of the scientific results that will be obtained by the Hera mission.

2 DATA SET DESCRIPTION

2.1 Didymos system spectra

A few spectroscopic ground-based observations of the Didymos system have been taken during its previous apparitions (Binzel et al. 2004a; De León et al. 2010; Kiersz et al. 2021; Ieva et al. 2022). Other observations were made before and after DART impact on 2022 September 26 (De León et al. 2023; Polishook et al. 2023). The spectra taken by Polishook et al. (2023) and De León et al. (2006, 2010) were used in this work, and they covered the 0.65–2.5 and 0.5–2.5 μm spectral ranges, respectively (Fig. 1). In Table 1, the observation characteristics of Didymos spectra are reported.

Furthermore, Polishook et al. (2023) took the spectra just before and right after the DART impact, and this will allow the identification of possible changes in the spectra due to the impact. These spectra show some differences in the slopes and band depths values of the two absorption bands that are compatible with a change in grain size and/or a change in space weathering degree (Brunetto et al. 2005; Strazzulla et al. 2005; Lantz et al. 2013; Palamakumbure et al. 2023; Fig. 1). The signal-to-noise ratio (SNR) of the three spectra was calculated across the whole spectra using the following relation:

$$\mathrm{NOISE} = \sqrt{\frac{\sum_i^N \left(y_i' - y_i\right)}{N}}$$

$$\mathrm{SNR} = \frac{\mathrm{SIGNAL}}{\mathrm{NOISE}},$$

where the signal is the spectrum smoothed over a boxcar of 17 that simulates the ideal noiseless spectrum. The SNR was found to be 33, 76, and 147 for the De León et al. (2010) and Polishook et al. (2023) pre-impact and post-impact spectra, respectively. In addition, the 2 μm absorption band of the pre-impact spectrum is very noisy at its depth. Therefore, we considered the post-impact spectrum for our analogue selection procedure. Following a private communication with David Polishook, it was necessary to remove the 0.65–0.75 μm range from the spectrum due to a non-linear response of the SpeX instrument (Table 2).

2.2 Meteorites spectra

To find the terrestrial analogous to the Didymos system, its spectrum was compared with the meteorites ones. For this purpose, we selected two spectral data bases: RELAB[1] and PSF[2]. RELAB has two operational spectrometers available to users: (1) a near-ultraviolet, visible, and near-infrared bidirectional spectrometer (0.3–2.6 μm) and (2) a near- and mid-infrared Fourier-transform infrared (FT-IR) spectrometer (0.8–200 μm).The PSF (Planetary Spectrophotometer Facility) spectral data, from the C-TAPE at the University of Winnipeg, used in this work were acquired using the ASD FieldSpecPro High Resolution spectrometer (0.35–2.5 μm). The data sets contain more than one thousand spectra of about three hundred different ordinary chondrites.

3 METHODS

This work is based on available observations (De León et al. 2006; Polishook et al. 2023) and previous spectral studies of Didymos and ordinary chondrites (De León et al. 2006, 2010; Dunn et al. 2010a,

[1] https://sites.brown.edu/relab/
[2] https://www.uwinnipeg.ca/c-tape/index.html

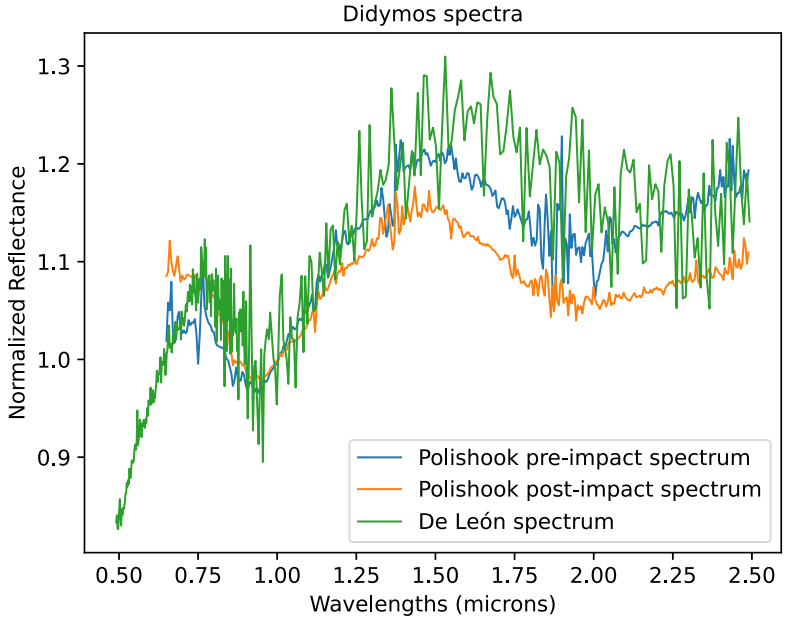

Figure 1 Didymos spectra normalized at 1 μm taken by De León et al. (2010) and Polishook et al. (2023).

Table 1 Observation characteristics of Didymos spectra.

Spectrum name	Observing date	Airmass	r(au)	Δ(au)	$\alpha(^\circ)$	V-mag.
Polishook pre-impact (Polishook et al. 2023)	2022 Sep 26	1.68	1.047	0.076	53	14.55
Polishook post-impact (Polishook et al. 2023)	2022 Sep 27	1.65	1.044	0.075	54	14.56
De Leon spectrum[3] (De León et al. 2010)	2004 Jan 16	1.07	1.280	0.330	22.8	17.6

Table 2 Definition of the shoulders and trough of the absorption bands.

Spectral feature	Didymos	Meteorites
Left shoulder Band I	Taken at 0.75 μm	Taken at 0.75 μm
Right shoulder Band I	1.3–1.6 μm (polynomial fit)	0.95–1.8 μm
Band I trough	0.8–1.1 μm	0.8–1.2 μm
Left shoulder Band II	1.3–1.6 μm (polynomial fit)	0.95–1.8 μm
Right shoulder Band II	Taken at 2.5 μm	Taken at 2.5 μm
Band II trough	1.7–2.3 μm	1.8–2.5 μm

2013; Cheng et al. 2018; Rivkin et al. 2023). In the next paragraphs, we will define and calculate the key spectral features of Didymos and meteorites spectra that will be used to perform the selection of the best analogues. In the following, we will refer to the absorption bands at 1 and 2 μm as Band I and Band II, respectively.

3.1 Analysis of didymos spectrum

In order to select the best analogues, we compared the spectral parameters of Didymos with those of the considered meteorites.[3] The spectrum was initially smoothed over a boxcar of 17 spectral bands. Then, the band centres of Band I and Band II were calculated as

[3]This spectrum was taken with two different telescopes NOT (Nordic Optical Telescope) and TNG (Telescopio Nazionale Galileo) for the visible and the near infrared part, respectively. The values reported in the table are a mean of the characteristics of the two portions of the spectrum.

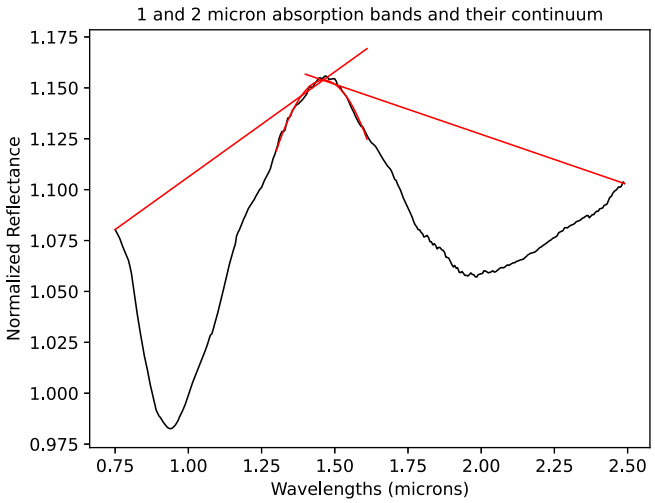

Figure 2 Didymos post-impact smoothed spectrum and its absorption bands continuum and shoulder polynomial fit superimposed.

the minimum of the absorption bands after the continuum correction (Cloutis et al. 1986; Clark 1999; Fig. 2). The continuum is defined as the line linking the absorption band shoulders maximum (Cloutis et al. 1986). The right shoulder of Band I was defined as the second-order polynomial fit of the spectrum between 1.3 and 1.6 μm, and the left shoulder is not completely defined as the spectrum is truncated at 0.75 μm; therefore, its maximum was taken as the reflectance value at 0.75 μm. The left shoulder of Band II is coincident with the right one of Band I, while the right shoulder is not completely defined as the

spectrum is truncated at 2.5 μm; therefore, its maximum was taken as the reflectance value at 2.5 μm. The band troughs, defined between 0.8 and 1.1 μm for Band I and between 1.7 and 2.3 μm for Band II, were then divided by the continuum, following a similar procedure shown in Longobardo et al. (2014) and Massa et al. (2023,2024). Finally, the absorption bands were found to be centred at 0.945 and 1.945 μm, respectively.

The uncertainty on the band centres was calculated in four steps:

1. Calculation of the polynomial fits error as the standard deviation

$$\sigma = \sqrt{\frac{\sum_{i=1}^{N} \left(x_i' - x_i\right)^2}{N - M}}, \quad (1)$$

where x_i' and x_i are the reflectance of the polynomial fit and the smoothed spectrum, respectively, and *N*–*M* is the degree of freedom of the fit (Taylor et al. 1982);

2. Calculation of the continuum error as the root mean square error between the continuum calculated as the line linking the shoulders maximum and the one calculated as the line linking the shoulder maximum plus their error;

3. Propagation of the previously calculated errors on the continuum corrected absorption band;

4. Definition of the band centre error range considering the reflectance values near the band centre and their error.

The procedure described above led to an error range of (0.935, 0.96) μm for the band centred at 0.945 μm and of (1.925, 1.985) μm for that centred at 1.945 μm.

Due to the large initial data set, the band centre alone is not sufficient to identify the best analogues, so it was necessary to define other parameters: the slope and the band depth of the two absorption bands. Differently than band centre, these two parameters are in general influenced by the space weathering and the grain size of Didymos (Brunetto et al. 2005; Strazzulla et al. 2005; Lantz et al. 2013; Palamakumbure et al. 2023), and this will be included in our selection (see next section).

The slopes were defined as the slope of the continuum of Band I and Band II, and they were found to be 0.102 and −0.050, respectively. The error on the slopes is very low compared to its value, and thus it is negligible.

The band depth can be calculated through the following relation (Clark et al. 1984):

$$\mathrm{BD} = 1 - \frac{R_c}{R_{con}},$$

where R_c and R_{con} are the measured reflectance and the calculated continuum reflectance at the band centre, respectively. The band depths were found to be 0.108 and 0.063 for Band I and Band II, respectively. The error on the band depths is very low compared to its value, and thus it is negligible.

The parameters calculated on the post-impact spectrum were also calculated on the one taken by De León et al. (2010). This spectrum was much different in global shape and seemed to show a Band I centre at longer wavelengths compared to those taken by Polishook et al. (2023). The Band I centre was found to be at 0.978 μm with an error range of (0.945, 1.02). Also, the band centre of the 2 μm band was found to be at much longer wavelengths, and its right shoulder is very difficult to define, differently from the most recent spectra in which the right shoulder is partially visible. All these examinations confirmed the initial idea of discarding this spectrum.

3.2 Analysis of meteorites spectra

The meteorites spectra used in this work were taken from the RELAB and PSF spectral data bases. First, we selected only the ordinary chondrites spectra. The spectra were then normalized at 1 μm as that of Didymos, and only the ones defined at least in the spectral range of Didymos spectrum were selected. The laboratory spectra were smoothed with a boxcar of seven spectral bands in order to remove possible spikes. Finally, the meteorites spectra were cut between 0.75 and 2.5 μm in order to have the same spectral range as Didymos and to apply the same analysis procedure.

The calculation of the shoulders of the two absorption bands was redefined for meteorites spectra due to the different spectral resolution and SNR ratio with respect to Didymos. The right shoulder of the Band I was defined between 0.95 and 1.8 μm and is coincident with the left shoulder of the Band II. The left shoulder of the Band I and the right shoulder of the Band II were truncated at 0.75 and 2.5 μm, respectively, and the maximum of the shoulders were chosen as the reflectance values at 0.75 and 2.5 μm, respectively, as was done for Didymos. The band troughs were defined between 0.8 and 1.2 μm for the Band I and between 1.8 and 2.5 μm for the Band II. Finally, the band centre, slope, and band depth were calculated in the same way as Didymos. All the spectral parameters calculated on the meteorites are generally influenced by grain size (Ueda et al. 2002; Cloutis et al. 2015; Bowen et al. 2023). This problem was not addressed in this work because Didymos grain size is unknown (this is true in particular for the post-impact spectrum, which is mainly due to the DART impact ejecta characterized by a very large and unknown grain size distribution), but its possible influence on the analogue selection will be discussed in the conclusion section.

4 RESULTS AND DISCUSSION

4.1 Analogues selection

The Didymos analogues selection was based on the spectral parameters defined in Section 3. The first selection was made using the band centres value because, for this work, they have a negligible variation with space weathering and grain size changes (Brunetto et al. 2005; Sanchez et al. 2012; Lantz et al. 2013; Cloutis et al. 2015; Bowen et al. 2023; Palamakumbure et al. 2023), so it is the most reliable parameter. We selected all the meteorites with band centres values consistent with Didymos ones within the error ranges. The resulting data set was reduced by more than a half compared to the initial one, composed of more than one thousand spectra of ordinary chondrites.

The second selection was based on band depths and slopes and was performed on the data set that emerged from the first selection. Since these two parameters are defined on Didymos spectrum with a negligible error, it was necessary to define a procedure in order to compare the values. A 4D space parameter was defined, where the slope and the band depth of Band I and Band II are used as dimensions. The best analogues are the ones closest to Didymos in the 4D space. For this purpose, a new metric tensor was defined in this space as:

$$g = \begin{pmatrix} 1/\mathrm{slope1}^2 & & & \\ & 1/\mathrm{slope2}^2 & & \\ & & 1/\mathrm{banddepth1}^2 & \\ & & & 1/\mathrm{banddepth2}^2 \end{pmatrix},$$

where slope1, slope2, banddepth1, and banddepth2 are the ones calculated on Didymos spectrum.

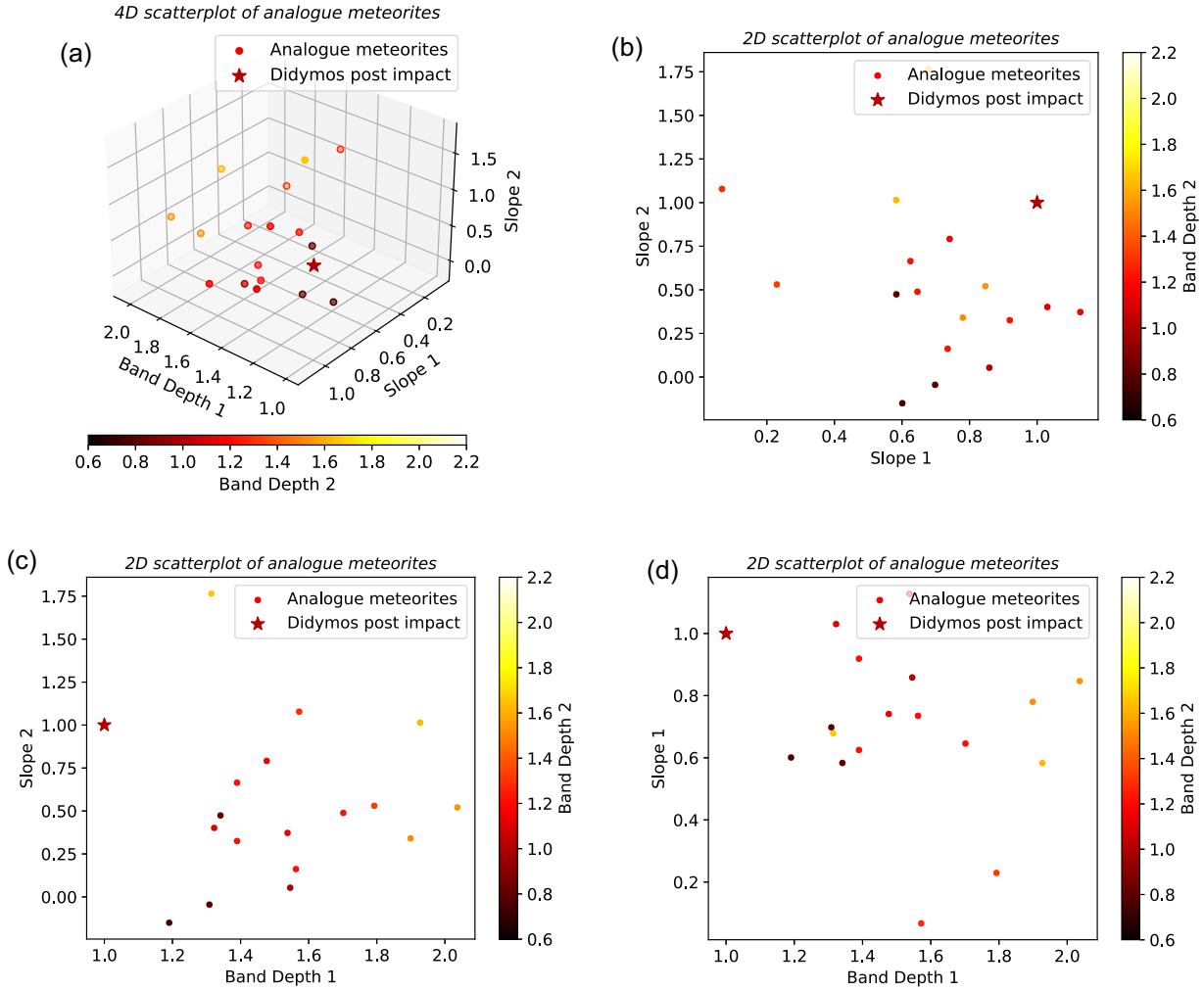

Figure 3 (a) 4D scatterplot of analogue meteorites, the star symbol represents Didymos post-impact. (b), (c), (d) 2D scatterplots showing different projections of the 4D scatterplot.

This metric allowed us to set up a distance measure that will result to be normalized to the values of Didymos parameters (Carroll 2004; Kreyszig 2013). Through the metric tensor $g_{\mu\nu}$, it is possible to define the length of an infinitesimal displacement $d\boldsymbol{q}$ in this 4D space, which will be written in the form:

$$ds^2 = g_{\mu\nu} dq^{\mu} dq^{\nu}. \tag{2}$$

In the case under examination, $d\boldsymbol{q}$ becomes $\boldsymbol{q}$ that represents the distance between Didymos, placed at $\boldsymbol{r} = (\text{slope1}, \text{slope2}, \text{banddepth1}, \text{banddepth2})$ and a random meteorite placed in this space $\boldsymbol{r'} = (\text{slope1}', \text{slope2}', \text{banddepth1}', \text{banddepth2}')$ such that $\boldsymbol{q} = \boldsymbol{r'} - \boldsymbol{r} = (\text{slope1} - \text{slope1}', \text{slope2} - \text{slope2}', \text{banddepth1} - \text{banddepth1}', \text{banddepth2} - \text{banddepth2}')$. Thus, equation (2) becomes

$$\begin{aligned} s^2 = {} & \frac{1}{\text{slope1}^2} * \left(\text{slope1} - \text{slope1}'\right) 2 + \frac{1}{\text{slope2}^2} \\ & * \left(\text{slope2} - \text{slope2}'\right) 2 + \frac{1}{\text{banddepth1}^2} \\ & * \left(\text{banddepth1} - \text{banddepth1}'\right) 2 + \frac{1}{\text{bandddepth2}^2} \\ & * \left(\text{banddepth2} - \text{banddepth2}'\right) 2 \, , \end{aligned}$$

where the root of s^2 is the distance between the two points. The distance was measured between Didymos and all meteorites selected based on the band centre. The meteorites closest to Didymos (i.e. with the lowest distance) were selected as analogues (Fig. 3). Finally, to avoid terrestrial weathering, only the 'Fall' type of meteorites was considered, i.e. meteorites that were found right after falling on Earth. The selection was truncated at the maximum distance of 1.25, i.e. the distance in 4D space between the parameters calculated on Didymos post-impact spectrum and the ones calculated on the pre-impact spectrum (banddepth1, bandepth2, slope1, slope2 = 0.102, 0.066, 0.217, −0.024); this was done to consider all the meteorites within the fluctuation of Didymos spectrum across the impact, shown in the spectra in Fig. 1 and in the spectra of De León et al. (2023). These fluctuations may be attributed both to differences in space weathering and grain size, and also to differences in the phase angle between Didymos and the meteorites spectra. This procedure made it possible to come up with a list of about 17 spectra of 13 meteorites (Table 3). In general, there can be multiple spectra of the same meteorite inside the data bases; a multiple selection of different spectra from different data bases of the same meteorite reinforces its analogy with Didymos, because it implies that different spectra taken from different scientists with different facilities on different samples of the same meteorites were selected. In Table 3, the column 'number

Table 3 Table of meteorites analogous to Didymos. The notes are those reported in the data bases.

Meteorite name	Sub-type	Distance	Grain size (microns)	Number of selections	Data base	$\frac{olv}{olv+pyx}$	Notes
Aldsworth	LL5	0.60	0–150	1	RELAB	0.58	–
Saratov	L4	0.67	Unsorted	2	PSF	0.53	–
		0.81	Unsorted		RELAB	0.56	
Rio Negro	L4	0.69	25–250	1	RELAB	0.54	–
Mezo-Madaras	L3	0.77	0–125	1	RELAB	0.60	–
Hamlet	LL4	0.85	0–150	2	RELAB	0.58	–
		1.20	Unsorted		PSF	0.56	
Hedjaz	L3–6	0.96	0–125	1	RELAB	0.58	–
Chelyabinsk	LL5	1.07	0–125	1	RELAB	0.56	–
C3-1							
Krymka	LL3	1.10	20–250	2	RELAB	0.55	Bulk sample
		1.15	20–250		RELAB	0.58	Dark powder
Soko-Banja	LL4	1.10	Unsorted	1	RELAB	0.43	–
Paragould	LL5	1.13	25–250	1	RELAB	0.55	100 per cent Light (L) T. S. 2286–2 Black Chondrite
Molina	L5	1.17	Unsorted	1	PSF	0.57	–
Bald Mountain	L4	1.20	Unsorted	1	PSF	0.56	–
Cynthiana	L4	1.21	Unsorted	2	PSF	0.60	–
		1.24	0–125		RELAB	0.58	

of selections' indicates how many spectra of the same meteorite were selected, and the column 'data base' indicates the data base from which it was taken.

We performed a statistical analysis of the meteorites sub-types. From Table 3, the selected meteorites are divided into L: LL: H = 9 : 8 : 0, but this statistic needs to be corrected for a possible bias induced by data bases imbalance between the different sub-types. Indeed, considering all the OCs in the data bases, the initial sub-types proportion is L: LL: H = 2.5 : 1 : 1.52. Dividing the proportion found in Table 3 by the initial proportion of the OCs, we obtain a normalized proportion that is L: LL: H = 0.31 : 0.69 : 0. This implies that Didymos matches the LL, L, and H sub-types spectra at 69 per cent, 31 per cent, and 0 per cent, respectively. Finally, the best OC sub-types that match with Didymos are the L/LL ones with a preference for the LL type; this agrees with and reinforces the result found by Dunn et al. (2013), Ieva et al. (2022), and Rivkin et al. (2023).

4.2 Evaluation of observational geometry role

The observation conditions of Didymos are reported in Table 1, while the selected meteorites (Table 3) have all been observed at a 30° phase angle. The difference in the phase angle between Didymos spectrum and the meteorites is 24°. In order to evaluate how this difference in phase angle affects our results, we suppose that the photometric behaviour of Didymos is similar to that of other S-type asteroids such as Eros or silicates-dominated asteroids such as Vesta (due to a lack of photometric studies on Didymos). Based on this, the silicates band depths and centres can be considered independent of a variation of 24° of the phase angle (Sanchez et al. 2012; Longobardo et al. 2014), unless there is a contamination of darkening agents such as carbonaceous chondrites and metals that are expected to be contained in low amounts in OC L and LL sub-types, that are considered to be representative of Didymos composition (Dunn et al. 2010a, 2013; this work). The slope variation can be evaluated by considering the ratio of the reflectance values at 0.946, 1.932, and 1.486 μm on Eros (Clark et al. 2002). The variation of the ratio of the reflectance at 1.486 and 0.946 μm gives an indication of the variation of the slope and of the band depth (since 0.946 μm is localized at the depth of the absorption bands), and it varies by 2.9 per cent when going from 30° to 55° of phase angle and by 5.0 per cent from the pre- to post-impact spectrum of Didymos (Clark et al. 2002). The ratio of the reflectance values at 1.932 and 0.946 μm gives an indication of the slope variation (since the two values are both contained in the depth of the absorption bands), and it varies by 2.4 per cent when going from 30° to 50° phase angles and by 6.4 per cent from the pre- to the post-impact spectrum of Didymos (Clark et al. 2002). This means that the photometric influence due to the difference in the phase angle between Didymos and the meteorites spectra is contained in the fluctuation of Didymos pre- and post-impact spectra.

Moreover, photometric variations of S-type asteroids are expected to be lower in ground observation than in space-resolved observations because the phase curve slope of a body increases with increasing the spatial resolution of the data (Longobardo et al. 2016).

For all these reasons, we can neglect the role of phase angle variations between the Didymos systems and ordinary chondrites under the assumption that the photometric behaviour of Didymos is similar to that of other S-type and/or silicate asteroids.

4.3 Taxonomical classification

Furthermore, based on the recent spectrum of Didymos, it is possible to improve its classification. Following the classification scheme of DeMeo et al. (2014), Didymos is classified as an S-type asteroid due to its band minimum below 0.96 μm, unlike what was done by Cheng et al. (2018), in which the band minimum was higher than 0.96 μm, which is the minimum requirement to be considered as an Sq-type asteroid (DeMeo et al. 2014). This is in agreement with previous classifications of Didymos (De León et al. 2006; Polishook et al. 2023).

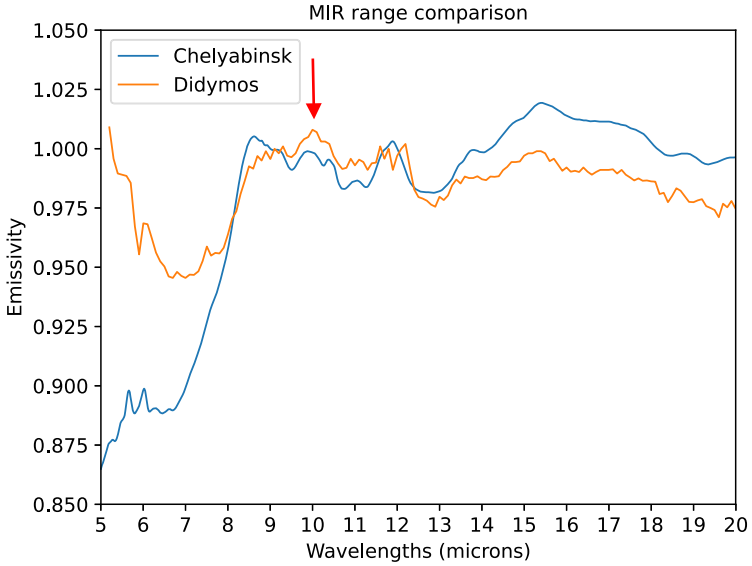

Figure 4 Comparison between Chelyabinsk and Didymos spectra in the MIR range (Rivkin et al. 2023). The arrow indicates the emissivity feature at 10 μm. The spectra are normalized at 9 μm.

Table 4 Table of the best meteorites analogous to Didymos. The table is ordered in descending order of matching.

Analogue names	Sub-type	Distance	Multiple selection	Multiple selection from different data bases	Selected in literature	Match in the MIR range
Saratov	L4	0.67 to 0.81	X	X	–	–
Hamlet	LL4	0.85 to 1.20	X	X	X	–
Cynthiana	L4	1.21 to 1.24	X	X	–	–
Chelyabinsk	LL5	1.07	–	–	–	X
Rio Negro	L4	0.69	–	–	X	–
Aldsworth	LL5	0.60	–	–	–	–

4.4 Comparison with the MIR spectral range and final selection of the analogues

Rivkin et al. (2023) found a mismatch in the MIR range between Didymos and the OC meteorites regarding the absence of an emissivity feature near 10 μm and a drop in the emissivity between 9 and 14 μm in the meteorites. A better match with Didymos was obtained using an OC with a grain size of <25 μm, but despite that, the mismatch described before was still present. Most of the meteorites spectra in the online data bases only span the VIS–NIR range. Despite that, we found one meteorite (Chelyabinsk) from Table 3 whose spectrum also spans the MIR range. Fig. 4 shows the meteorite emissivity spectrum obtained through Kirchhoff's Law (Hapke 2012), which allows the emissivity to be calculated from the reflectance, in which the feature near 10 μm is present along with the other features and a general match about the emissivity level in the entire MIR range between Chelyabinsk and Didymos (Fig. 4). The meteorite particle size shown in Fig. 4 is <125 μm; this implies that the mismatch found in Rivkin et al. (2023) was not to be only addressed to the particle size but also to the composition of the samples used. Finally, this result supports the analogy between the composition of the meteorites selected in this work and that of the Didymos system.

4.5 Didymos composition inferred from the selected meteorites

The ordinary chondrites are characterized by the presence of both olivine and pyroxene, whose spectral features fall in the 1 μm, and 1 and 2 μm regions, respectively. The ratio of the Band I and II areas (BAR) was previously used to estimate the olivine and pyroxene relative abundances from the OC meteorites spectra (Cloutis et al. 1986; Dunn et al. 2010b). The composition of the analogue meteorites can be derived using the following linear relation between the BAR and the olv/(olv + pyx) modal ratio (Dunn et al. 2010b):

$$\frac{\text{olv}}{\text{olv}+\text{pyx}} = -0.242 * \text{BAR} + 0.728. \quad (3)$$

The mean value of the olv/(olv + pyx) modal ratio reported in Table 3 is 0.56 and its standard deviation, calculated with equation (1), is 0.04. In the hypothesis that these meteorites are indeed representative of Didymos composition, this value can be considered the modal ratio of Didymos, and it is in agreement with those calculated in the same way by Rivkin et al. (2023) and Dunn et al. (2013) on its spectrum (0.57 ± 0.16 and 0.61 ± 0.03, respectively) taken by *JWST* and a ground-based observatory (De León et al. 2010), respectively.

5 CONCLUSIONS

The analogues selection performed by Ieva et al. (2022) was made using a chi-square minimization of the VIS spectra of Didymos and the meteorites, whereas in this work a VIS–NIR spectrum of Didymos was used, and the selection was based on the comparison between spectral parameters that are highly indicative of the asteroid composition.

The terrestrial meteorites spectrally analogous to Didymos were searched throughout the PSF and RELAB data bases. The meteorites that were found to be analogous to Didymos are listed in Table 3 and are sorted in ascending order of distance between Didymos and the meteorites in the 4D space. In Table 3, the ordinary chondrites spectra can be divided, based on their sub-types, into 8 LL, 9 L, and 0 H. A statistical analysis based on the OC sub-types showed that Didymos matches the LL, L, and H sub-types spectra at 69 per cent, 31 per cent, and 0 per cent, respectively. This also suggests that Didymos may be composed of both LL and L ordinary chondrites.

The number of meteorites in Table 3 is still large; another selection based on another criterion can be made. To identify the best analogues, we considered, in order of importance, the distance, the selection of spectrum from different data bases, the number of selections, the match with Didymos in the MIR range, and eventually a comparison with the literature. The best analogues are reported in Table 4.

It is worth underlining that multiple selection is an important parameter to consider, but it is not sufficient to discard a meteorite because there may be meteorites whose spectrum is contained just once in the data bases.

Since the grain size is not known on Didymos, especially after the resurfacing occurred due to DART impact, it was not possible to consider the grain size as a parameter for the selection procedure. Indeed, the selection shown in Table 3 is influenced by the meteorites grain size. Nevertheless, it can be used to estimate the Didymos system mean grain size. In particular, if a selected meteorite is produced with a grain size that differs from those reported in the table, it is possible that its spectral parameters change, and thus its distance from Didymos may change. This means that a meteorite can be considered a good analogue only if we assume that its grain size is similar to that of Didymos. Therefore, a further selection based on grain size can be made in the future after assessing this parameter on Didymos system.

The comparison in the MIR range between the Didymos spectrum and a meteorite from Table 3 shows that there is also a match in the MIR range, differently than Rivkin et al. (2023), and it strengthens the relation between Didymos and the analogue meteorites identified in this work.

The modal ratio of olv/(olv + pyx) abundance of the Didymos system is found to be 0.56 ± 0.04; this result is a fundamental improvement of previous measurements (Dunn et al. 2013; Rivkin et al. 2023) and can give information about the Didymos evolutionary scenario.

The meteorites identified in this work will also be used for calibration purposes by the VISTA, ASPECT, Hyperscout H, and TIRI payloads scientific teams. Furthermore, they will be used to retrieve spectral parameters helpful to the future analysis of Hera data, to make a first guess about the composition of Didymos system through X-Ray diffraction (XRD) analysis of the samples, and also to understand the influence of space weathering on the meteorites and thus on Didymos.

ACKNOWLEDGEMENTS

This work was funded through the ASI (Italian Space Agency) - UNIBO (University of Bologna) agreement 2022–8-HH.0 and the INAF (National Institute of Astrophysics) 2023 Mini-Grants Program.

DATA AVAILABILITY

The data underlying the MIR analysis in this article are available in the Mikulski Archive for Space Telescopes (MAST), at https://dx.doi.org/10.17909/9ymc-em60.
The (De León et al. 2006, 2010) Didymos spectrum is available at http://research.iac.es/proyecto/pcssolar/pages/en/data.php.
The post and pre-DART impact spectra of Didymos were published by Polishook et al. (2023).
This research utilizes spectra acquired with the NASA RELAB facility at Brown University (https://sites.brown.edu/relab/relab-spectral-database/) and others contained in the C-TAPE data base (of which Edward A. Cloutis is the director) at the University of Winnipeg (https://www.uwinnipeg.ca/c-tape/sample-database.html).

REFERENCES

Adams J. B., 1974, J. Geophys. Res., 79, 4829
Binzel R. P., Rivkin A. S., Stuart J. S., Harris A. W., Bus S. J., Burbine T. H., 2004a, Icarus, 170, 259
Binzel R. P., Perozzi E., Rivkin A. S., Rossi A., Harris A. W., Bus S. J., Valsecchi G. B., Slivan S. M., 2004b, Meteorit. Planet. Sci., 39, 351
Bowen B. et al., 2023. Planet. Sci. J., 4, 52
Brunetto R., Strazzulla G., 2005, Icarus, 179, 265
Carroll S. M., 2019, Spacetime and Geometry: An Introduction to General Relativity. Cambridge University Press, Cambridge
Cheng A. F. et al., 2018, Planet. Space Sci., 157, 104
Clark B. E. et al., 2002, Icarus, 155, 189
Clark R. N., 1999, in Rencz A.N., ed., Manual of Remote Sensing: Remote Sensing for the Earth Sciences, Spectroscopy of Rocks and Minerals, and Principles of Spectroscopy. John Wiley and Sons, New York, p. 3
Clark R. N., Roush T. L., 1984, J. Geophys. Res., 89, 6329
Cloutis E. A., Gaffey M. J., Jackowski T. L., Reed K. L., 1986, J. Geophys. Res., 91, 11641
Cloutis E. A. et al., 2015, Icarus, 252, 39
De León J., Licandro J., Duffard R., Serra-Ricart M., 2006, Adv. Space Res., 37, 178
De León J., Licandro J., Serra-Ricart M., Pinilla-Alonso N., Campins H., 2010, A&A, 517, A23
De León J. et al., 2023. ACM Conf., LPI Contrib. No. 2851, Spectral Characterization of Didymos During the DART Impact. Flagstaff, Arizona/Virtual, p. 2372
DeMeo F. E., Binzel R. P., Lockhart M., 2014, Icarus, 227, 112
Dunn T. L., Cressey G., McSween H. Y., McCoy T. J., 2010a, Meteorit. Planet. Sci., 45, 123
Dunn T. L., McCoy T. J., Sunshine J. M., McSween H. Y., Jr, 2010b, Icarus, 208, 789
Dunn T. L., Burbine T. H., Bottke W. F., Jr, Clark J. P., 2013, Icarus, 222, 273
Grady M. M., Pratesi G., Cecchi V. M., 2014, Atlas of Meteorites. Cambridge Univ. Press, Cambridge, p. 71
Hapke B., 2012, Theory of Reflectance and Emittance Spectroscopy. Cambridge Univ. Press, Cambridge, p. 469
Ieva S. et al., 2022, Planet. Sci. J., 3, 183
Kiersz D. A., Green S. F., Rivkin A. S., Fitzsimmons A., Seccull T., 2021, 7th IAA Planetary Defense Conf., Spectroscopic Observations of (65803) Didymos with VLT/X-Shooter. Vienna, Austria, p. 194
Kreyszig E., 2013, Differential Geometry. Courier Corporation, Chelmsford, MA, US
Lantz C., Clark B. E., Barucci M. A., Lauretta D. S., 2013, A&A, 554, A138

Longobardo A. et al., 2014, Icarus, 240, 20
Longobardo A. et al., 2016. Icarus, 267, 204
Massa G. et al., 2023, Universe, 9, 296
Massa G. et al., 2024, Icarus, 409, 115870
Michel P. et al., 2018, Adv. Space Res., 62, 2261
Michel P. et al., 2022, Planet. Sci. J., 3, 160
Naidu S. P. et al., 2020, Icarus, 348, 113777
Okada T. et al., 2022, LPI Contrib. No. 2678, 53rd Lunar and Planetary Science Conference, Development of Thermal Infrared Multiband Imager TIRI for Hera Mission. The Woodlands, Texas, p. 1319
Pajola M. et al., 2022, Planet. Sci. J., 3, 210
Palamakumbure L., Mizohata K., Flanderová K., Korda D., Penttilä A., Kohout T., 2023, Planet. Sci. J., 4, 72
Polishook D., DeMeo F. E., Burt B. J., Thomas C. A., Rivkin A. S., Sanchez J. A., Reddy V., 2023, Planet. Sci. J., 4, 229
Raducan S.-D., Jutzi M., Zhang Y., Ormö J., Michel P., 2022, A&A, 665, L10
Rivkin A. S. et al., 2023, Planet. Sci. J., 4, 214
Sanchez J. A., Reddy V., Nathues A., Cloutis E. A., Mann P., Hiesinger H., 2012, Icarus, 220, 36
Strazzulla G., Dotto E., Binzel R., Brunetto R., Barucci M. A., Blanco A., Orofino V., 2005, Icarus, 174, 31
Sultana R. et al., 2023, Icarus, 395, 115492
Taylor J. R., William T., 1982, An Introduction to Error Analysis: the Study of Uncertainties in Physical Measurements. University Science Books, Mill Valley, CA, p. 45
Ueda Y. et al., 2002. 33rd Annual Lunar and Planetary Science Conference, Changes of Band I Center and Band II/Band I Area Ratio in Reflectance Spectra of Olivine-Pyroxene Mixtures due to the Space Weathering and Grain Size Effects. Houston, Texas, p. 2023
Vernazza P. et al., 2012, Icarus, 221, 1162

This paper has been typeset from a TEX/LATEX file prepared by the author.